NEAR FIELD ACOUSTIC MICROSCOPY

B.T. Khuri-Yakub, S. Akamine, B. Hadimioglu[†], H. Yamada[*] and C.F. Quate

Edward L. Ginzton Laboratory
Stanford University
Stanford, CA 94305 U. S. A.

[†]Xerox Palo Alto Research Center
3333 Coyote Hill Road
Palo Alto, CA 94304 U.S.A.

[*]Quantum Metrology Department
National Research Laboratory of Metrology
1-1-4 Umezono
Tsukuba 305, Japan

ABSTRACT

We have integrated silicon micromachining techniques with piezoelectric thin film deposition to make a near-field acoustic microscope. A piezoelectric zinc oxide (ZnO) transducer is deposited on a substrate of 7740 glass. A sharp tip is formed in a silicon wafer which is anodically bonded to the glass substrate. A sample is attached to substrate of glass with a receiving ZnO transducer. The transducer on the tip excites an ultrasonic beam which passes from the tip to the sample and is detected by the receiving transducer. A feedback signal is generated to keep the transmitted amplitude constant as a sample is raster scanned. The feedback signal is applied to a tube scanner and is also used to modulate the intensity of a display monitor. We find that the instrument has a vertical height sensitivity of about 20Å, and a lateral resolution of better than 800Å.

INTRODUCTION

In traditional imaging systems, coherent radiation is focused to a diffraction limited spot. Electron microscopes, optical microscopes, and acoustic microscopes are a few examples of such instruments. Near filed imaging refers to a means of obtaining a resolution that is superior to the diffraction limit, the so-called "super resolution."[1] The near field optical microscope,[2,3,4] near field acoustic microscope,[5,6] and the scanning tunneling[7] and atomic force microscopes[8] are examples of such instruments. Here, the resolution is determined by the size of an aperture or tip that is far smaller than the wavelength of the radiation. The tunneling acoustic microscope is designed and operated in this regime.

Takata et al.[9] at Hitachi have already demonstrated a variation of the TAM. They combined the tunneling and acoustic devices by vibrating the tip at 70 KHz. Their detector was a piezoelectric element attached to the back surface of the sample. They mapped the distribution of elastic properties by scanning the vibrating tip over the surface. The resolution was limited to a few hundred Angstroms. Uozumi et al.[10] added a piezoelectric transducer on the base of the tip. The transducer operated at a frequency of 1.2 MHz. Variations in the amplitude and phase of the

signal reflected from the end of the tip were measured as the tip was scanned over the sample. Again, a spatial resolution of the order of 100 Å was achieved.

In our version of the near field scanning acoustic microscope, we integrate a piezoelectric transducer with a sharp tip using silicon integrated circuit processing technology. Such a configuration allows us to operate at higher frequencies and obtain better vertical and horizontal resolutions. Also, this integration would allow us the use of combined modes of operation with a scanning tunneling microscope (STM) or atomic force microscope (AFM).

SYSTEM CONFIGURATION

The near-field acoustic microscope consists of an acoustic transducer and tip assembly which together form an acoustic source smaller than the acoustic wavelength (Figure 1). A sample is imaged by scanning the tip in a raster fashion and measuring the transmitted acoustic signal. A feedback signal keeps the transmitted acoustic signal constant by changing the spacing between the tip and the sample. Using this technique we image both conducting and insulating samples using acoustic impedance and height variations as contrast mechanisms.
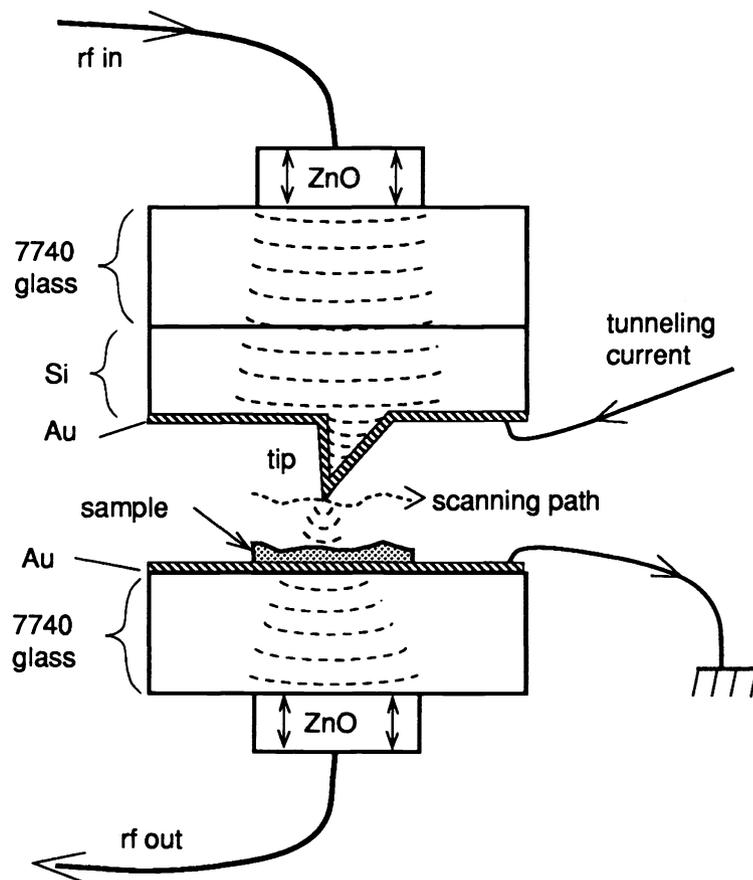

Fig. 1 Schematic diagram of transducer-tip assmebly.

Construction of the near-field acoustic microscope is divided into two distinct categories: the mechanical instrument and the microfabricated tip/transducer assembly. The mechanical instrument and control electronics are identical to those used in STM and described

elsewhere[11,12,13]. Our version utilizes a tripod design[14] which allows control of separation between the tip and the sample as well as their relative tilt (Figure 2).
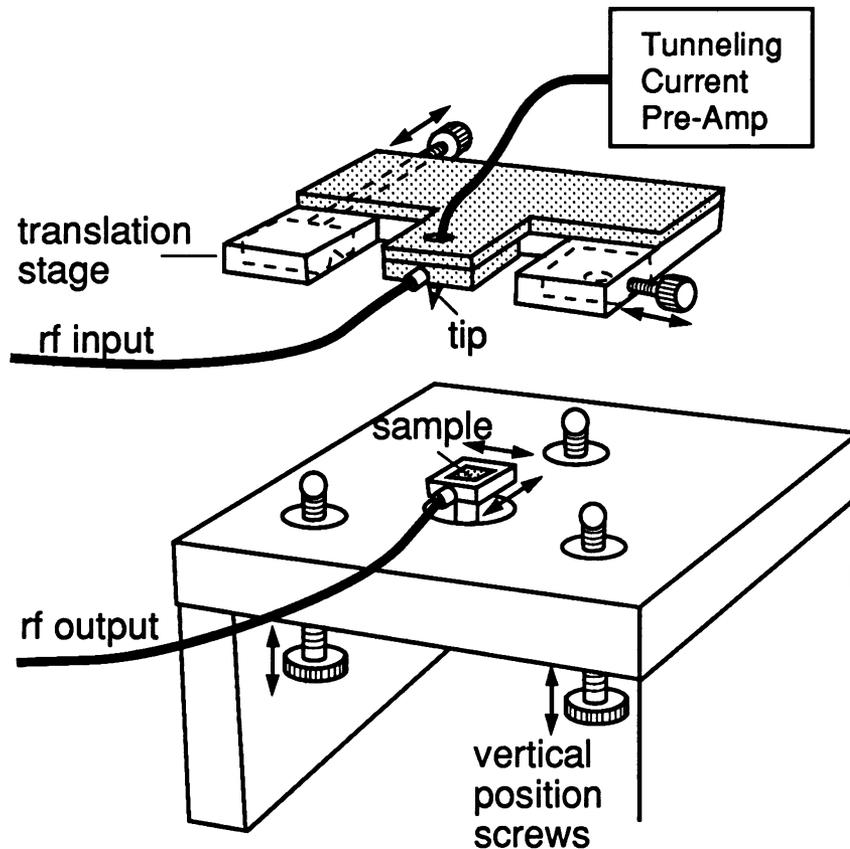

Fig. 2 Schematic diagram of the mechanical scanning system.

The essential feature of the microfabricated tip/transducer assembly is a sharp silicon tip. While several methods for fabricating sharp tips are known [15,16], we use a tetrahedral, single crystal silicon tip. The fabrication process for the tetrahedral tips is outlined in Figure 3. The process begins with the formation of vertical-walled silicon posts using dry etching. A nitride covered silicon wafer is used so that the resulting post is capped with nitride while its sidewalls are bare silicon. The post is shaped so that a sharp corner is pointing in the [110] direction of the wafer. Utilizing a LOCOS process, several thousand angstroms of oxide are then grown at low temperatures (950° C) so that the sidewalls of the post are protected by oxide whereas the top of the post is still capped by nitride. The nitride cap is selectively removed using a reactive ion plasma of SF_6 and CF_3Br. The exposed silicon in the center of the post is etched in an anisotropic silicon etchant such as EDP or KOH. Most of the post's interior is etched away during this step with the exception of small tetrahedral volumes in the corners of the post. These tetrahedral volumes are not etched since they are bounded on their sides by oxide and on one face by a (111) crystallographic plane. A finished tip is shown in Figure 4.
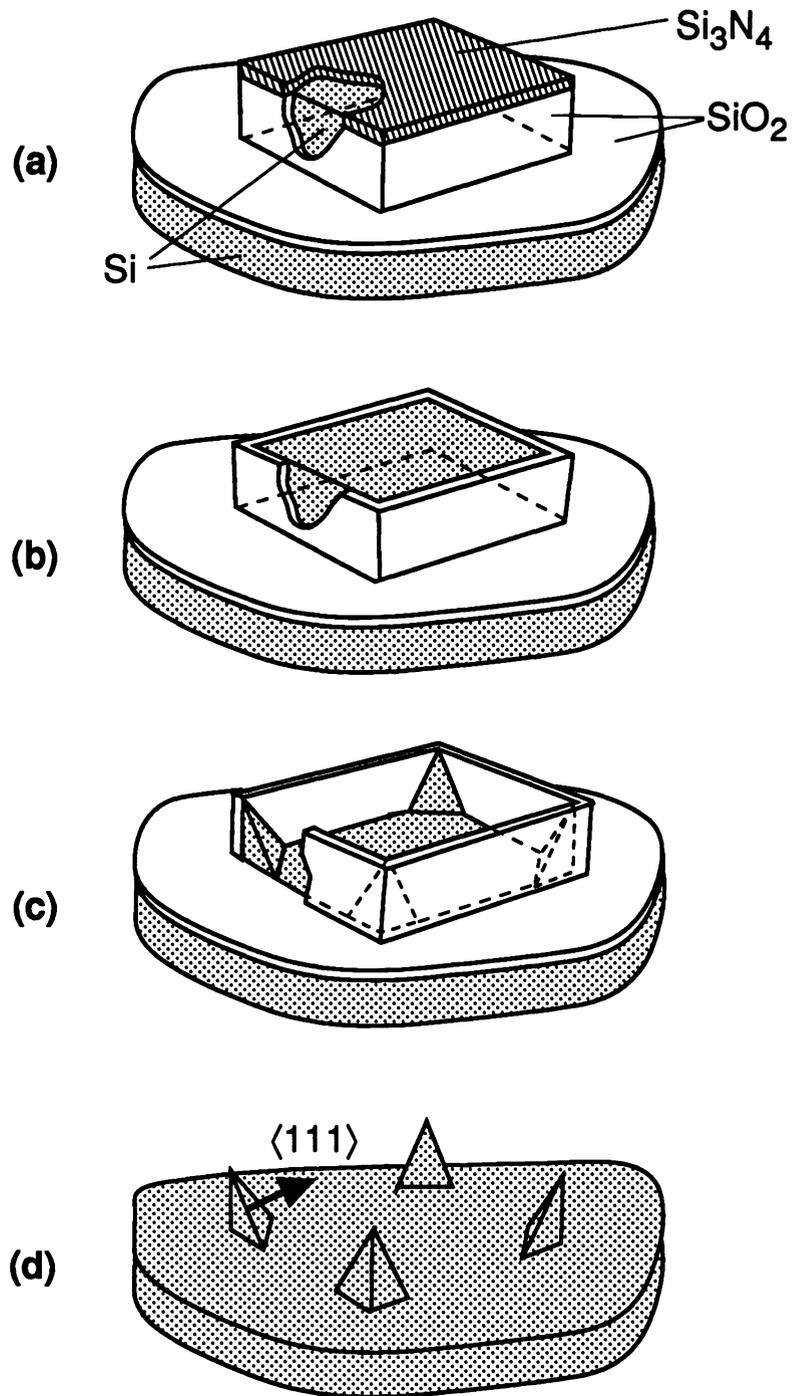
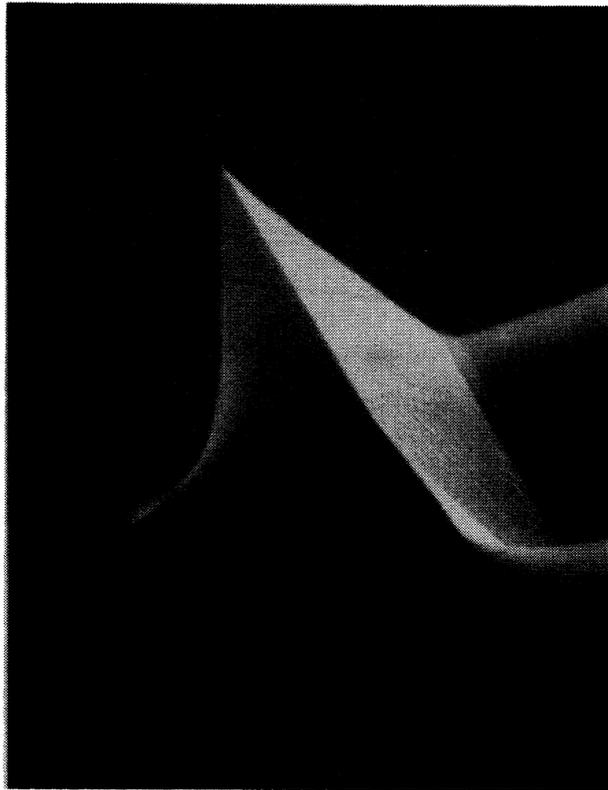Figure 3. Process outline for making tetrahedral silicon tips.

Figure 4. A tetrahedral silicon tip.

We favor this tip fabrication technique because it is quite easy to execute. There are no critical time dependant etches nor exotic materials to consider. Tips made in this way have radii of curvature typically less than 500 Å and as low as 200 Å. A key factor in the sharpness of these tips is the low temperature oxidation step which is inherent in the process. The relatively high stress in the low temperature oxide causes sharpening of silicon features. Thus, even though the original silicon post has corners whose sharpness is limited by the resolution of the lithography, the final sharpness is determined by the sharpening effect of the low temperature oxidation [16,17].

The ultrasonic transducer uses a sputtered zinc oxide (ZnO) film as the piezoelectric element. The ZnO is sandwiched between two Cr/Au and Ti/Au electrodes forming a 50 x 200 μm transducer with a resonant frequency at 175 MHz. The resonant frequency is determined by the thickness of the ZnO and Au films. The transducers were electrically tuned to operate at a frequency of 135 MHz. The substrate for the transducer is Corning 7740 glass, chosen to be compatible with silicon during a subsequent anodic bonding step.

After fabrication, the tip and the transducer are aligned using a two-sided aligner. A special jig protects the tip at all times. The aligned pieces are then heated to 325° C on a hot plate and anodically bonded for 15 to 30 minutes with 1500 -2500 V applied.

MEASUREMENT SYTEM

A schematic of the electronic measurement system is shown in Fig.5. It combines a superheterodyne detection system with the scanning and height control electronics of a STM. An rf tone burst at the frequency of operation is amplified and applied to the transmitting transducer

which is brought into contact with the sample. The detected tone burst is amplified, gated, mixed with a local oscillator, and passed through a diode detector then a signal averager to improve the signal to noise ratio. Typically, the transmitting transducer is excited with a 1 watt peak power. The total dynamic range of our system excluding the signal averager is 120 dBs. The one way insertion loss of a transducer is typically 14 dBs.

The signal is used in a feed back loop to control the Z-motion of a cylindrical tube scanner, and also to modulate the intensity of a display monitor. Thus, images are generated by scanning a sample and using the feedback signal to modulate the intensity of the display monitor at the location of the tip. The contrast in the images is due to changes in the detected signal caused by both acoustic impedance and height variations.
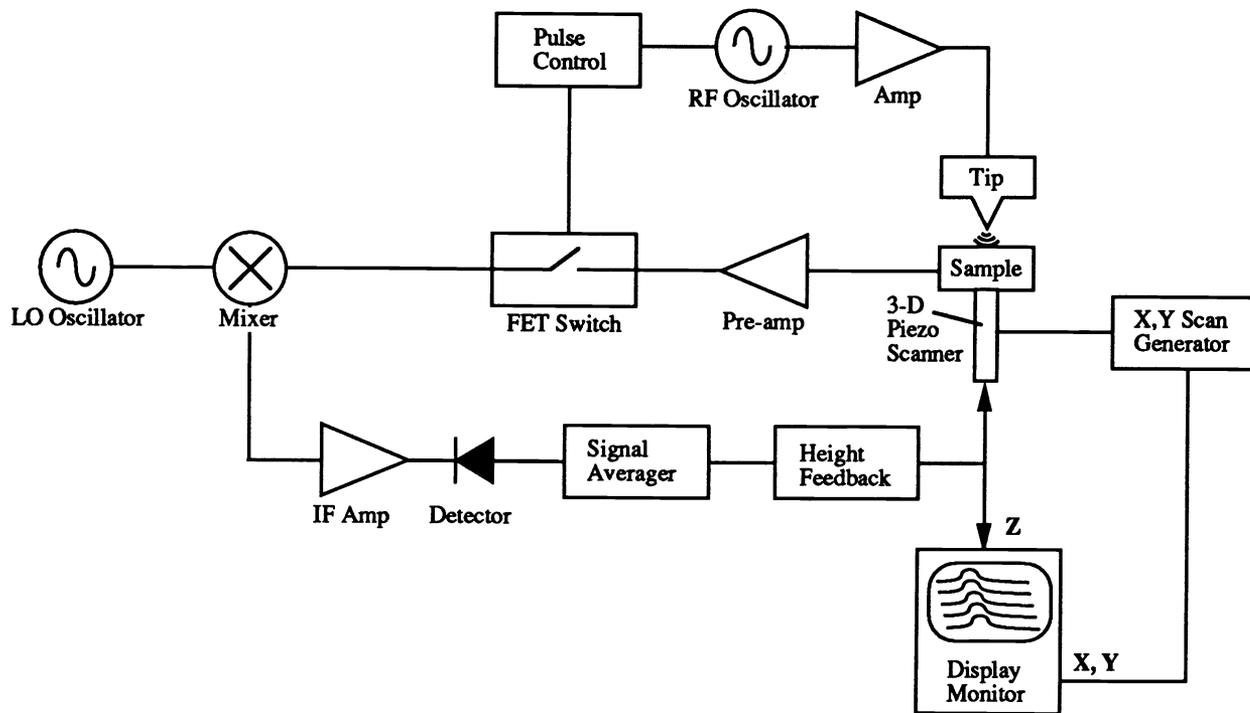
Fig.5 Schematic diagram of the near filed acoustic microscope

EXPERIMENTAL RESULTS

The experiments are carried out by placing a sample on a bare ultrasonic receiver which is identical to the tip transducer except for the lack of a tip. We have used 1000 Å evaporated gold films on Corning 7740 glass as a sample as well as an anodically bonded silicon grating. The sample is mounted on a piezoelectric tube scanner commonly used in STMs.[18] The tip transducer is mounted in the microscope head and is held firmly by a kinematic seating arrangement.

In order to align the transmitting tip transducer to the receiving sample transducer, water is first placed in the gap between the tip and sample. A 135 MHz pulsed signal is applied to the tip transducer and the tip is moved in X and Y to maximize the transmitted signal. The amplitude of the transmitted signal is also highly sensitive to tilt so tilt is also optimized by using the tripod screws. When the transmitted signal has been maximized, the water in the gap is removed and the tip is approached to the sample.

Two simple experiments have been conducted. The first was to measure the transmitted signal intensity versus gap spacing and the second was to scan the sample under the tip to try to obtain a topographic image of the sample surface. The first experiment was carried out by putting a modulation of approximately 1000 Å on the sample height. The sample was moved toward and away from the tip at 1 to 10 Hz while the transmitted signal was monitored. At large gap spacings, no signal was detected. Upon approaching the tip to the sample, the transmitted signal increased in correspondence to the tip position. Figure 6 shows a clear knee in the curve where the transmission begins and increases as the tip is brought closer to the sample. At these signal levels, we can detect a 20 Å excursion in the gap spacing at a unity signal to noise ratio.
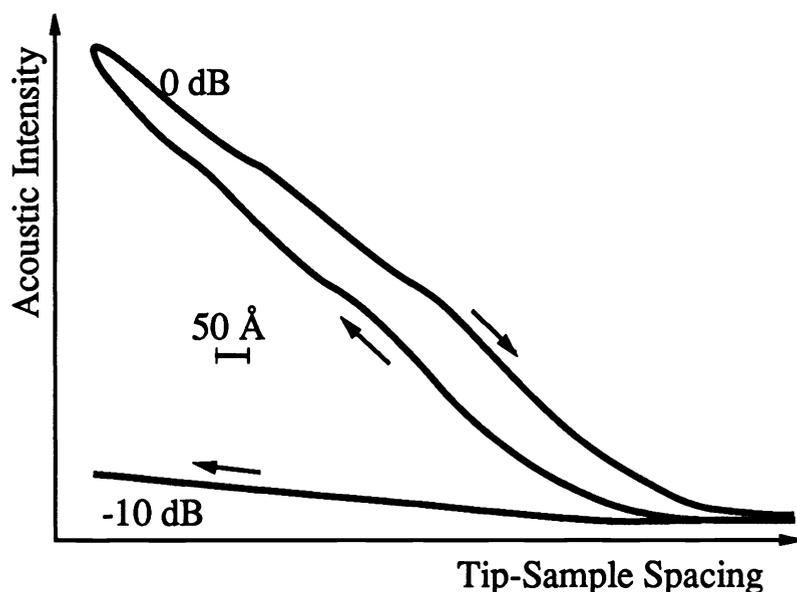

Figure 6. Transmitted acoustic signal intensity plotted versus tip/sample separation.

A one-dimensional topograph of the glass surface of the sample transducer was obtained by scanning the sample under the tip using height feedback to maintain constant transmitted signal intensity (Figure 7). The upper curve shows a 4000 Å scan of a region and the lower scan shows the same region scanning a range twice as small. For a particular tip these scans are reproducible and repeated scans over the same region show the topography is unchanged. There is significant variation from tip to tip however and degradation in tip performance is observed after hard crashes into the sample.
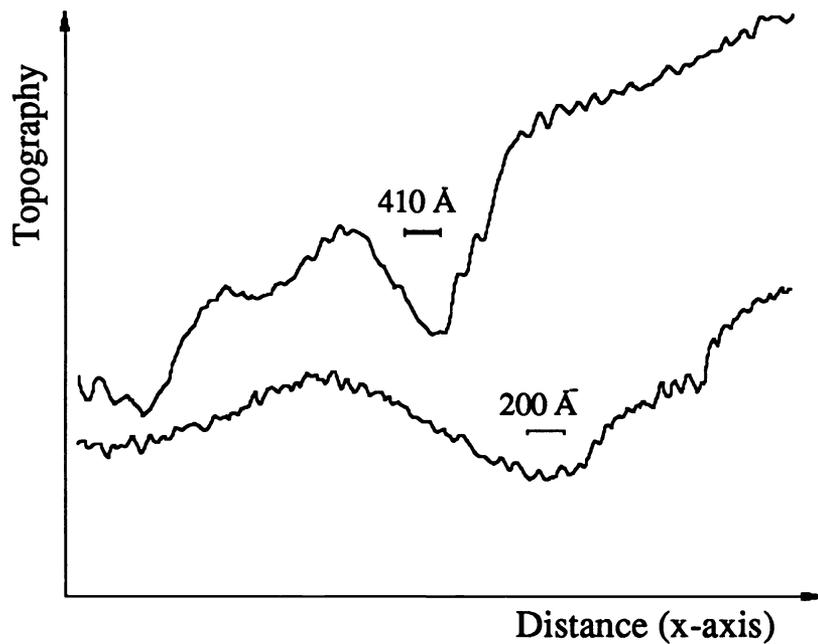
Figure 7. One-dimensional topography of gold film on glass imaged using feedback to maintain constant transmitted signal intensity.

Fig.8 shows an image of a 6.5 μm grating in a silicon sample. The grating is formed by etching grooves 1.5 μm wide, 1000 Å deep in the silicon sample.
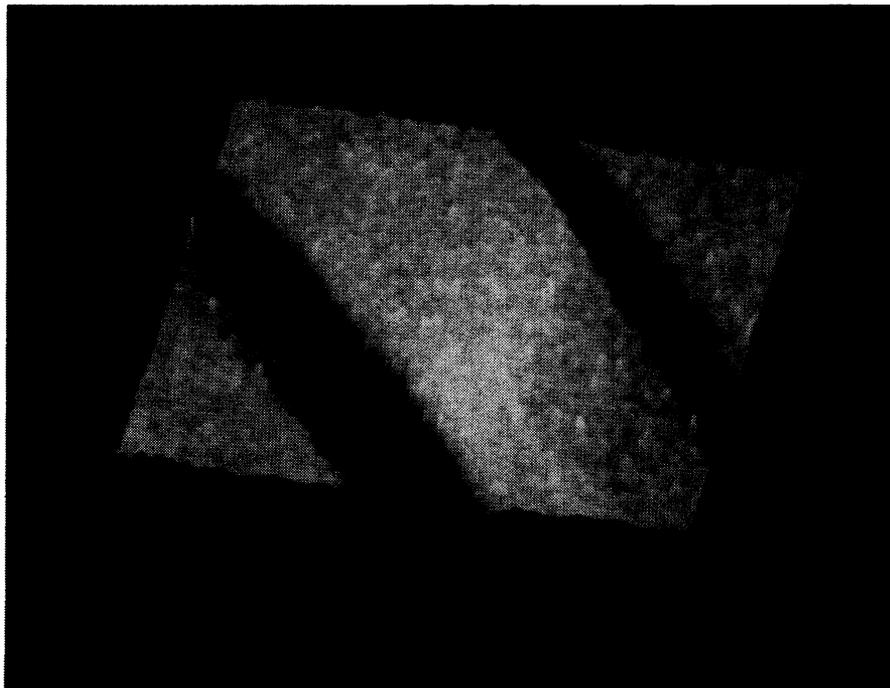

Fig.8 Image of a 6.5μm grating in silicon.

DISCUSSION

The results of these experiments indicate that it is possible to transmit acoustic waves from one transducer to another through a point junction. Using an excitation of 135 MHz results in wavelengths on the order of 60 μm in silicon. Nonetheless we are transmitting this signal through a tip with radius of curvature of hundreds or perhaps a few thousand angstroms.

The actual mode of transmission is as yet unclear. Since the experiments were all conducted in air, it is assumed that all surfaces have a contamination layer which may be as thick as a few hundred angstroms. This soft contamination layer may partially explain the seemingly long range interaction of the tip and sample as seen in Figure 5. If the tip were simply crashing into the surface repeatedly, we would expect the location of the knee of the curve as well as the curve's slope to change over time. Instead, we observe that a given tip can be approached over 50 times and the curve does not change significantly. Variations in the curves are seen for different tips.

The one-dimensional scanning data is very interesting since it seems to show a lateral resolution of approximately 1000 Å. While this data was being taken, several parameters such as scan size, rotation, and frequency were varied to eliminate the possibility of scan artifacts. This resolution of about 1000 Å seems to be born out in the 2-D scan of the grating.

CONCLUSIONS

We have microfabricated a very sharp silicon tip and integrated it with a ZnO acoustic transducer. The LOCOS process for fabricating the tips is very simple to execute as it does not rely on any critical lithography or etching steps. A low temperature thermal oxidation step inherent in the process routinely sharpens the tips to radii of curvature 200 to 500 Å. These tips may find applications in microvacuum electronics and other scanning probe microscopes.

To operate the microscope, 135 MHz acoustic waves are launched into the tip from the ZnO transducer and transmitted down through the tip's apex and to a receiving transducer. Using this configuration, we have transmitted ultrasonic waves with a wavelength of 60 μm through a junction that is a few thousand angstroms or less in diameter.

Initial experiments monitoring the transmitted signal levels while modulating the gap separation indicate that a 20 Å variation in the tip sample separation can be detected. By feeding back on these transmitted signals we are able to maintain a fixed gap separation while the sample is scanned laterally under the tip. A one-dimensional scan has resolved 1000 Å features in a gold film on a glass surface. Since the acoustic wavelength is approximately 50 μm, we believe that the acoustic transmission we are observing is a near-field effect. Two-dimensional scans of etched silicon gratings in silicon indicate that a similar resolution of 1000 Å is also achieved.

Significant improvements must be made before this instrument can be used to image samples reliably. In addition, the exact nature of the acoustic coupling must be clarified and understood. For that purpose, tunneling current detection has to be included in order to measure the ultrasonic coupling before solid contact is made to the sample. For the same purpose, the signal to noise ratio needs improvement. These improvements will allow us to study variations in the mechanical properties of materials on the atomic scale.

References

1. E. A. Ash and G. Nichols, Nature, 237, 510-512 (1972).
2. D. W. Pohl, W. Denk, and M. Lanz, Appl. Phys. Lett. 44, 651-653 (1984).
3. A. Harootunian, E. Betzig, M. Isaacson, and A. Lewis, Appl. Phys. Lett. 49, 674-676 (1986).
4. K. Lieberman, S Harush, A. Lewis, and R. Kopelman, Science, 247, 59-61 (5 January 1990).
5. P. Guethner, E. Schreck, K. Dransfeld, and U. Ch. Fischer, NATO Workshop, Erice, Sicily, April 17-29, 1989, in *Scanning Tunneling Microscopy and Related Methods*, eds. R. J. Behm, N. Garcia and H. Roher, NATO ASI Series E: Applied Sciences, vol. 184, pp. 507-514, 1990 Kluwer Academic Publishers, The Netherlands.
6. B. T. Khuri-Yakub, C. Cinbis, C. H. Chou, and P. A. Reinholdtsen, Proceedings of the 1989 IEEE Ultrasonics Symposium, October 3-6, 1989, Montreal, Canada, pp. 805-807, IEEE No. 89CH2791-2, ISSN: 0090-5607.
7. G. Binnig, H. Rohrer, Ch. Gerber, and E. Weibel, Phys. Rev. Lett. 50, 120-123 (1983).
8. G. Binnig, C. F. Quate, and Ch. Gerber, Phys. Rev. Lett. 56, 930-933 (1986).
9. K. Takata, T. Hasegawa, S. Hosaka, S. Hosoki, and T. Komada, Appl. Phys. Lett. 55, 1718-1720 (23 October 1989).
10. K. Uozomi, and K.Yamamuro, Jpn. J. Appl. Phys. 28, No. 7, L1297-L1299 (July 1989).
11. S. I. Park, and C. F. Quate, Rev. Sci Inst. 58, 2010 (1987).
12. C. F. Quate, Physics Today 39, 26 (1986).
13. P. K. Hansma, V. B. Eilings, O. Marti, and C. E. Bracker, Science 242, 209 (1988).
14. K. Besocke, Surf. Sci. Tech. 181, 145 (1987)
15. T. R. Albrecht, S. Akamine, T. E. Carver, and C. F. Quate, J. Vac. Sci. Technol. A 8, 3386, (1990).
16. R. B. Marcus, T. S. Ravi, T. Gmitter, K. Chin, D. Liu, W. J. Orvis, D. R. Ciarlo, C. E. Hunt, and J. Trujillo, Appl. Phys. Lett. 56, 236 (1990).
17. D. B. Kao, J. P. McVittie, W. D. Nix, and K. C. Saraswat, IEEE Trans. Electron Devices ED-35, 25 (1988).
18. G. Binnig, and D. P. E. Smith, Rev. Sci. Instrum. 57, 8 (1986).